Low-Overhead Scheduling for Synchronization in Large-Scale Digital Twin Systems

Zifan Zhou[*], Juaren Steiger[*], Yin Sun[†], and Bin Li[*]

[*]Department of Electrical Engineering, Pennsylvania State University, University Park, Pennsylvania, USA
[†] Department of Electrical and Computer Engineering, Auburn University, Alabama, USA

Abstract—Digital Twin (DT), where a twin world maintains virtual representations of entities in the physical world, is an emerging technology with applications in smart cities, intelligent traffic, and manufacturing. We study a large-scale DT system where numerous entities share a communication channel to report their states to a cloud server tasked with updating their virtual representations. Here, the state synchronization between physical and twin worlds can be effectively quantified by the Version Age of Information (VAoI), which measures the number of state updates yet to be replicated in the twin world. A scheduler tasked with determining which physical entity should transmit its state at any given time must therefore balance the tradeoff between VAoI and communication overhead. In this paper, we quantify the average VAoI and communication overhead for three scheduling policies from the literature: Randomized Scheduling, Round-Robin, and Power-of-d. To analyze the Power-of-d policy in a large-scale system, we use mean-field analysis. Furthermore, we develop the Threshold-Based Power-of-d policy by extending the Power-of-d policy to the case where entities only report their states when their VAoI exceeds a threshold. We show that this threshold can be tuned so that the system achieves lower average communication overhead than the previous policies and achieves a similar average VAoI to the Power-of-d policy. We validate our theoretical findings with extensive numerical simulations.

I. INTRODUCTION

We live in a world of ubiquitous interconnected wireless devices that drive various cyber-physical applications. Many of these applications fall under the umbrella of Digital Twin (DT), where a twin world maintains virtual representations of entities in the physical world to facilitate real-time monitoring, collaboration, and risk-free experimentation. DT is an emerging technology that has garnered significant attention in recent years, inspiring a wide range of innovative studies that provide practical solutions for large-scale real-world applications [1]–[4] such as smart cities [5], intelligent traffic [6], and manufacturing [7]. A DT system typically consists of three main components: physical entities, virtual representations, and bidirectional information feedback links, as Fig. 1 shows. The physical entities (such as vehicles, buildings, etc.) serve as data sources, providing the latest state of relevant features (e.g., speed, temperature, etc.) to the cloud server. These data enable the creation of a twin world, offering deeper insights into the corresponding physical world and facilitating improved analysis and decision-making.

The complete and timely transmission of the latest data from physical entities is essential for achieving an accurate virtual representation and an efficient system. However, due to the limited communication resources and the computing capacity of the cloud server, achieving perfect real-time synchronization without data loss between numerous physical entities and their virtual representations is neither feasible nor practical. Therefore, a key challenge in large-scale DT systems is how to enhance operational efficiency and allocate the constrained network resources in a manner that minimizes the lag of state synchronization between the physical and twin worlds [8].

In this paper, we study the challenges of state synchronization and communication overhead optimization in large-scale DT systems. For state synchronization, the *age of information* (AoI) has recently been widely used as the optimized metric to evaluate the system performance [9]–[14]. The AoI of a virtual representation in a DT system can be defined as the time elapsed since its most recent successful state updates (e.g., [9], [15], [16] and see [17] for an overview). Although extensive research has focused on the analysis and optimization of AoI under various scenarios, a high AoI does not necessarily indicate a large lag of state synchronization. For instance, when synchronizing a vehicle, if the vehicle is stationary (e.g., parked or waiting at a traffic light), certain states (e.g., position or speed) may remain unchanged even as the AoI increases. To address this issue, we adopt the concept of *Version Age of Information* (VAoI) [18], the discrete form of AoI, which counts the number of state changes that have not been replicated in the twin world. Compared with AoI, VAoI is a more accurate metric for quantifying the lag of state synchronization between the physical and twin worlds.

To achieve a high-performance large-scale DT system, it is ideal to prioritize updating the entity with the largest VAoI. However, two significant challenges arise: (1) each entity operates independently and is unaware of the state of other entities; and (2) requiring all entities to upload their states to the scheduler for selection would result in prohibitive communication overhead. This kind of dilemma is commonly encountered in queueing systems such as the supermarket queueing model in [19]. To achieve better synchronization performance with acceptable communication overhead, the Power-of-d scheduling policy is a well-established solution [20]–[22]. This method optimizes the overall system performance by randomly sampling the states of d entities and selecting the one most suitable for service. A detailed description and analysis can be found in Section IV-A.

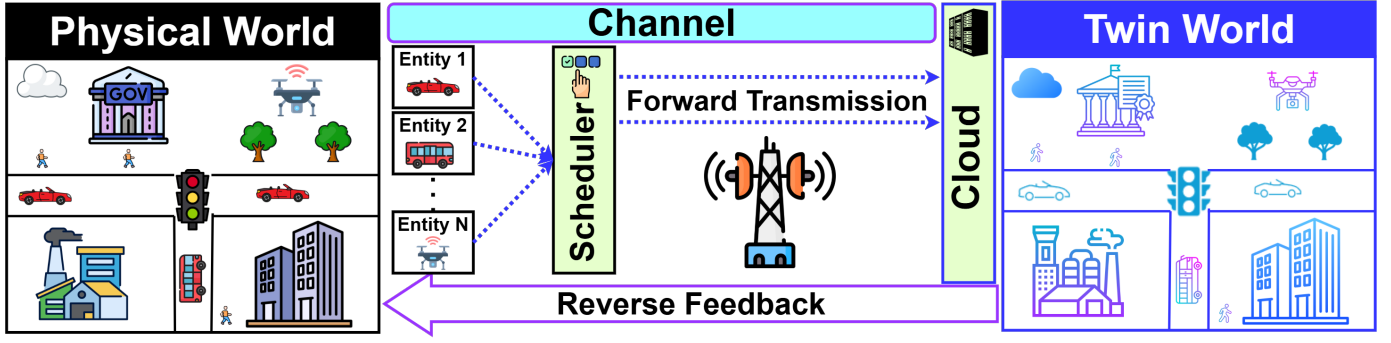Although the Power-of-d scheduling policy achieves bet-

Fig. 1: Large-Scale Digital Twin System: The physical world with real entities (left), the twin world with virtual representations (right), and bidirectional information feedback (center).

ter overall performance than other policies, it also leads to unnecessary communication overhead. The underlying reason is that entities passively accept upload commands without any awareness of their state. An intuitive solution is to allow entities to selectively accept or reject upload commands. The threshold policy, which has been widely studied and recently integrated with AoI in various scheduling scenarios [23]–[25], provides a framework where the scheduler uses a reasonable threshold to decide when or which entity should be scheduled. In this work, we propose a novel Threshold-based Power-of-d scheduling policy, which reduces the average VAoI compared to the Randomized and Round-Robin scheduling policy, while also lowering communication overhead compared to the Power-of-d and Max-VAoI scheduling policy.

To compare the overall performance of different policies, we convert the average VAoI and communication overhead into expressions based on the steady-state distribution by modeling the state transitions of entities as a Continuous Time Markov Chain (CTMC) and solving it by mean-field analysis. In this process, we assume an idealized large-scale DT system of infinite size, where the number of entities goes to infinity [21], [22], [26], [27]. Although the analysis is conducted in this ideal case, the simulation results closely align with the theoretical outcomes, validating the correctness of our assumption. Our main contributions are:

- We first present the model of a large-scale DT system comprising many physical entities, a shared communication channel, and a cloud server. The system can be viewed as a queueing model with a very large number of queues, thus enabling the mean-field analysis.
- Next, we carry out the probabilistic analysis of the Randomized and Round-Robin scheduling policies and mean-field analysis for the Power-of-d scheduling policy, then derive mathematical expressions for the average VAoI and average communication overhead.
- Then, we propose a new Threshold-based Power-of-d scheduling policy, which significantly reduces communication overhead while maintaining a comparable average VAoI to the Power-of-d policy. We also quantify the reduction in average communication overhead and analyze the impact of system and algorithm parameters on both

average VAoI and communication overhead.

- Finally, we conduct extensive simulations to validate our theoretical analysis. The results demonstrate that our policy perfectly achieves low lag of state synchronization with less communication overhead, making it highly suitable for large-scale DT systems.

II. SYSTEM MODEL

We consider a DT system consisting of N physical entities and a cloud server that tracks the states of entities (e.g., vehicle position and velocity in a DT-enabled smart city), enabling the DT operation via high-fidelity simulations, analysis, and decision-making. We assume that each entity independently updates its state according to a Poisson process with the same rate $\lambda > 0$, retaining the most recent updates and discarding the old ones. All entities share a common communication channel to transmit their states to the cloud server. Here, we assume that the twin world can update only one entity's state at a time and thus only one entity is allowed to transmit its state to the twin world at each scheduling instant. The service time for each scheduled entity follows an independent exponential distribution with rate $N\mu$.

Let $Q_n(t)$ denote the VAoI of physical entity n at time t, which measures the number of state changes of the nth physical entity at time t since its most recent successful state transmission to the cloud server. Thus, the VAoI more accurately captures the lag of state synchronization between the physical entity and its virtual representation compared to the traditional AoI, which only measures the time elapsed since the last successful transmission.
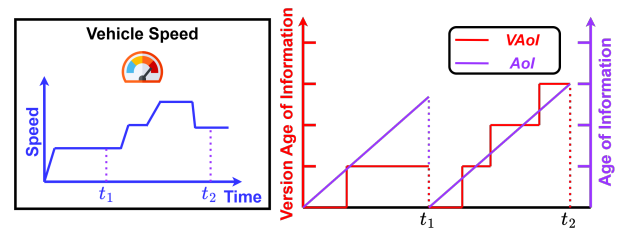

Fig. 2: Evolution of VAoI and AoI of physical entity n.

Fig. 2 illustrates the sample paths of the VAoI and AoI for n^{th} physical entity, where t_i denotes the time of the ith successful state transmission. Notably, the VAoI remains unchanged until t_1, whereas the AoI continues to increase until t_1, even though the state of physical entity n does not change. In general, a higher VAoI indicates a greater lag of state synchronization. Our goal is to design a scheduling policy that minimizes the average VAoI for each entity.

Although Randomized and Round-Robin scheduling policies achieve zero communication overhead, as the scheduler does not require any information from physical entities to make scheduling decisions, they lead to a high average VAoI, resulting in a large lag between the physical and twin worlds. To minimize the average VAoI, an intuitive approach is to schedule the physical entity with the largest VAoI to transmit its state. However, this requires all physical entities to report their states before the scheduler can make a decision, leading to significant communication overhead, especially when the number of entities N is large. This motivates us to design an efficient, low-overhead scheduling algorithm that achieves a favorable average VAoI. In this paper, we consider a class of scheduling policies under which the system achieves the steady state. Let $\overline{Q}^{(\pi)}$ and $\overline{C}^{(\pi)}$ be the average VAoI and communication overhead under scheduling policy π, respectively.

Next, we analyze the performance of both the Randomized and the Round-Robin scheduling policy, then compare them with the Max-VAoI scheduling policy through simulation. These baseline comparisons motivate the design of a new scheduling policy that achieves a low average VAoI with less communication overhead.

III. Evaluation of Baseline Scheduling Policies

In this section, we first evaluate the performance of the Randomized and the Round-Robin scheduling policy. Both policies operate with zero communication overhead, as the scheduler makes decisions independently, without receiving state reports from the physical entities. We then compare these two policies with the Max-VAoI scheduling policy that requires all physical entities to report their states before it makes the transmission decision via simulation to further clarify the motivation behind designing a new low communication overhead and low average VAoI scheduling policy.

A. Randomized Scheduling Policy

Under the Randomized scheduling policy, whenever the channel becomes available, one physical entity is selected uniformly at random to transmit its state. Consequently, the VAoI for each physical entity evolves as a Markov Chain. The state updates follow a Poisson process with rate λ, while the service time is exponentially distributed with rate μ, as illustrated in Fig. 3. Let $\pi_m^{(R)}$ denote the stationary probability that the VAoI is m under the Randomized scheduling policy. Solving the global balance equations gives $\pi_m^{(R)} = \frac{\lambda^m \mu}{(\lambda+\mu)^{m+1}}$

for all $m \geq 0$. Then the average VAoI $\overline{Q}^{(R)} \triangleq \sum_{m=0}^{\infty} m\,\pi_m^{(R)}$ of any physical entity is given by

$$\overline{Q}^{(R)} = \frac{\mu}{\lambda+\mu} \sum_{m=0}^{\infty} m \left(\frac{\lambda}{\lambda+\mu} \right)^m = \frac{\lambda}{\mu}. \qquad (1)$$

We can see from the above that the average VAoI increases linearly as the update rate increases, and decreases inversely as the service rate increases.
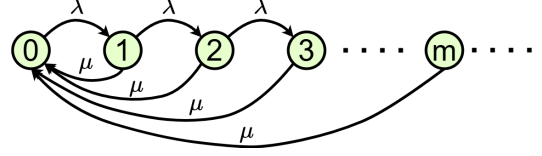

Fig. 3: The Markov chain representing a physical entity n's VAoI $Q_n(t)$ under the Randomized scheduling policy.

B. Round-Robin Scheduling Policy

Under the *Round-Robin* scheduling policy, in the kth scheduling instant, the scheduler schedules entity $n_k \triangleq ((k-1) \bmod N)+1$, i.e. the entities are scheduled cyclically. Unlike with the Randomized policy, we cannot directly analyze the system in steady state, and are therefore more interested in a limiting time-average. Let t_k denote the time at which the kth scheduling instant occurs. Note that as $N \to \infty$, $(t_{k+1} - t_k) \to 0$ almost surely for all k by the Borel-Cantelli lemma since $\Pr\{t_{k+1} - t_k > \varepsilon\} = e^{-N\mu\varepsilon}$ for all $\varepsilon > 0$. Then for a fixed entity n, considering a time-average that sums over discrete scheduling instants $t_n, t_{n+1}, \ldots$ approximates a continuous time-average well. In fact, we can show that

$$\widetilde{Q}_{n,L}^{(RR)} \triangleq \lim_{N \to \infty} \mathbb{E}\left[\frac{1}{LN} \sum_{j=n}^{LN+n-1} Q_n(t_j) \right] = \frac{\lambda}{2\mu} \qquad (2)$$

where $L \in \mathbb{Z}_+$ denotes the number of Round-Robin cycles under consideration. In order to derive (2), we introduce $U_n(T) \sim \text{Poisson}(\lambda T)$ to represent the number of times entity n updates its state during an interval of length T. The derivation is based on the following observations:

1) $n_k = n$ for all $k = \ell N + n$, where $\ell = 0, 1, 2, \ldots$
2) $Q_{n_k}(t_k) = 0$ and $Q_{n_k}(t_j) = U_{n_k}(t_j - t_k)$ for the next $N-1$ scheduling instants $j = k+1, k+2, \ldots, k+N-1$.
3) $(t_j - t_k) \sim \text{Erlang}(j - k, N\mu)$, and therefore $U_{n_k}(t_j - t_k) \sim \text{NegativeBinomial}\left(j - k, \frac{N\mu}{\lambda+N\mu}\right)$.

Also note that the mean of a random variable with NegativeBinomial$\left(j - k, \frac{N\mu}{\lambda+N\mu}\right)$ distribution is $\frac{\lambda(j-k)}{N\mu}$. Then

$$\left[\frac{1}{LN} \sum_{j=n}^{LN+n-1} Q_n(t_j) \right] = \frac{1}{L} \sum_{\ell=0}^{L-1} \frac{1}{N} \sum_{j=\ell N+n}^{(\ell+1)N+n-1} \mathbb{E}[Q_n(t_j)]$$

$$\overset{(a)}{=} \frac{1}{L} \sum_{\ell=0}^{L-1} \frac{1}{N} \sum_{j=1}^{N-1} \frac{\lambda j}{N\mu} = \left[\frac{N-1}{N} \right] \frac{\lambda}{2\mu} \to \frac{\lambda}{2\mu} \text{ as } N \to \infty$$

where (a) makes use of all three observations. The main takeaway here in the large-scale system is that the Round-Robin policy reduces the average VAoI by 50% compared to the Randomized policy.

C. Performance Comparison

We analyze two extreme scheduling policies that operate with zero communication overhead. While these policies minimize communication overhead, their performance in terms of average VAoI is suboptimal, where the Round-Robin scheduling policy achieves an average VAoI of approximately $\frac{\lambda}{2\mu}$ under large-system limitation. In contrast, the Max-VAoI scheduling policy can achieve a very small average VAoI by always selecting the most outdated physical entity. However, this policy requires all physical entities to upload their states to the scheduler, making it effectively a greedy approach. Due to its high communication overhead, it becomes impractical for large-system deployments. To illustrate the strengths and weaknesses of these scheduling policies, we present simulation results, highlighting their respective trade-offs.

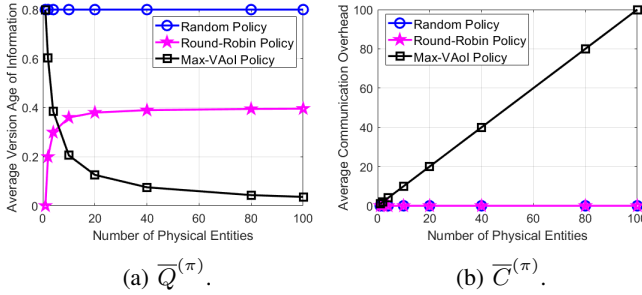(a) $\overline{Q}^{(\pi)}$. (b) $\overline{C}^{(\pi)}$.

Fig. 4: Comparison of different policies ($\lambda = 0.8$, $\mu = 1$).

The numerical results show that while the Round-Robin and Randomized scheduling policies are efficient in terms of communication overhead, the Max-VAoI scheduling policy exhibits a linear increase with the number of physical entities. For the average VAoI, we find that the Round-Robin policy achieves approximately half of the Randomized policy as the number of physical entities increases, yet both perform worse than the Max-VAoI scheduling policy, validating our theoretical analysis. These simulation results motivate us to explore whether it is possible to achieve a low average VAoI while simultaneously minimizing communication overhead.

Next, we introduce a classical algorithm in queueing theory named Power-of-d scheduling policy, which reduces the communication overhead and improves the system efficiency by randomly selecting d physical entities, obtaining their state information, and making scheduling decisions accordingly.

IV. Algorithm Design and Mean-Field Analysis

In this section, we first introduce the Power-of-d scheduling policy. It is quite challenging to directly analyze the Power-of-d policy due to the dependence among different physical entities. Fortunately, such a dependence vanishes in the large-system limit, allowing us to apply mean-field analysis. We then propose a new Threshold-based Power-of-d scheduling policy that simultaneously achieves the low average VAoI and low average communication overhead.

To proceed, we need to make the following *mean-field assumption* for the large-scale DT system as $N \to \infty$: any fixed number d of entities have independent VAoI, i.e.

$Q_1(t), Q_2(t), \ldots, Q_d(t)$ are mutually independent. This assumption relates to the core principle of mean-field analysis: that the behavior of the overall system is not noticeably influenced by any finite subset of its constituent entities. In the last section, the numerical results validate the correctness of theoretical results from the mean-field analysis.

A. Power-of-d Scheduling Policy

The Power-of-d scheduling policy operates as follows: At each scheduling instant t, the scheduler randomly issues d upload commands to d physical entities, which then report their current states to the scheduler. The scheduler then identifies the physical entity with the highest VAoI among them and allows it to transmit its state to the twin world. The VAoI of each physical entity forms an independent Markov Chain, as shown in Fig. 5.
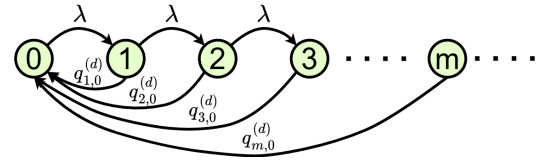

Fig. 5: The VAoI Markov Chain of a single physical entity in the large-system limit.

The transition rate $q_{m,0}^{(d)}$ represents the instantaneous rate of transitioning from state m to 0 while $\pi_m^{(d)}$ denotes the stationary probability of being in state m. Additionally, we define $S_m^{(d)} \triangleq \sum_{i=m}^{\infty} \pi_i^{(d)}$, where (d) represents the Power-of-d scheduling policy. We utilize the global balance equations to analyze the Markov Chain.

$$
\begin{cases}
\pi_0^{(d)}\lambda = \sum_{j=1}^{\infty} \pi_j^{(d)} q_{j,0}^{(d)} \\
\pi_m^{(d)}\lambda + \pi_m^{(d)} q_{m,0}^{(d)} = \pi_{m-1}^{(d)}\lambda, \text{ for } m = 1, 2, \ldots
\end{cases}
\tag{3}
$$

Proposition 1. *Under the Power-of-d scheduling policy, given the algorithm parameter d and system parameters λ and μ:*

(1) The distribution of the VAoI of the large-scale system in steady state is uniquely determined by the sequence of tail probabilities $\{S_m^{(d)}\}_{m \in \mathbb{Z}_{\geq 0}}$, where $S_0^{(d)} = 1$ and $S_m^{(d)}$ for $m > 0$ can be calculated iteratively using the equation

$$
\mu[1 - (1 - S_m^{(d)})^d] + S_m^{(d)}\lambda = S_{m-1}^{(d)}\lambda.
\tag{4}
$$

Moreover, $S_m^{(d+1)} < S_m^{(d)}$ for all $m, d \in \mathbb{Z}_+$ and therefore by the tail-sum formula for expectation,

$$
\overline{Q}^{(d+1)} = \sum_{m=1}^{\infty} S_m^{(d+1)} < \sum_{m=1}^{\infty} S_m^{(d)} = \overline{Q}^{(d)}.
\tag{5}
$$

Note that the above series converges since $\overline{Q}^{(1)} = \overline{Q}^{(R)}$.

(2) The average communication overhead is given by

$$
\overline{C}^{(d)} = d.
\tag{6}
$$

Proof. $q_{m,0}^{(d)}$ and $S_m^{(d)}$ have the following relationship:

Lemma 1. *The transition rate $q_{m,0}^{(d)}$ can be expressed as*

$$q_{m,0}^{(d)} = \frac{\mu}{\pi_m^{(d)}}[(1 - S_{m+1}^{(d)})^d - (1 - S_m^{(d)})^d]. \tag{7}$$

The detailed proof of this lemma can be found in Appendix A of our technical report [28].

According to Lemma 1, the global balance equation $\pi_m^{(d)}\lambda + \pi_m^{(d)}q_{m,0}^{(d)} = \pi_{m-1}^{(d)}\lambda$, and the fact that $\pi_m^{(d)} = S_m^{(d)} - S_{m+1}^{(d)}$, we have

$$\mu[(1 - S_{m+1}^{(d)})^d - (1 - S_m^{(d)})^d] + (S_m^{(d)} - S_{m+1}^{(d)})\lambda$$
$$= (S_{m-1}^{(d)} - S_m^{(d)})\lambda. \tag{8}$$

Summing both sides of the above equation gives

$$\sum_{j=m}^{\infty} \mu[(1 - S_{j+1}^{(d)})^d - (1 - S_j^{(d)})^d] + (S_j^{(d)} - S_{j+1}^{(d)})\lambda$$
$$= \sum_{j=m}^{\infty} (S_{j-1}^{(d)} - S_j^{(d)})\lambda = (S_{m-1}^{(d)} - S_{\infty}^{(d)})\lambda \tag{9}$$
$$= \mu[(1 - S_{\infty}^{(d)})^d - (1 - S_m^{(d)})^d] + (S_m^{(d)} - S_{\infty}^{(d)})\lambda$$

where $S_{\infty}^{(d)} \triangleq \lim_{j \to \infty} S_j^{(d)} = 0$. It follows that

$$\mu[1 - (1 - S_m^{(d)})^d] + S_m^{(d)}\lambda = S_{m-1}^{(d)}\lambda \tag{10}$$

The proof of Eq.(5) is a special case of the proof for Eq.(13) and is provided in Appendix B of our technical report [28].

For part (2), the average communication overhead $\overline{C}^{(d)} = d$ is given by simply noticing that the scheduler always selects d entities to report their states in each scheduling instant. □

Remark 1. *The theoretical analysis of the impact of d on $\overline{Q}^{(d)}$ aligns with intuitive expectations. As d increases, the scheduler has a higher probability of selecting a physical entity with a higher VAoI at each scheduling instant. This, in turn, enhances the likelihood of transmitting the most outdated states, thereby reducing the average VAoI. It is also evident that as d increases, the system requires more communication overhead because the scheduler must collect state reports from more physical entities.*

B. Threshold-based Power-of-d Scheduling Policy

In the aforementioned policy, the physical entity always passively accepts the upload command from the scheduler. However, in reality, the scheduler is unaware of the real state of each entity before issuing the command, which leads to unnecessary communication overhead. Our motivation is to enable the entity to selectively accept the upload command, thereby reducing this communication overhead. In other words, each physical entity has a consciousness of its own.

Physical entity consciousness: An intuitive method to quantify consciousness is setting a specified threshold (γ_n) for each physical entity n. In our Threshold-based Power-of-d scheduling policy, at each scheduling instant, the scheduler randomly sends d upload commands to physical entities with equal probability. Each selected physical entity then decides

whether to report its state to the scheduler. Finally, the scheduler selects one of the reporting physical entities with the maximal VAoI for service. The logistics of our policy are illustrated in Algorithm 1. In the homogeneous case, the threshold should be the same for all physical entities, denoted by γ. We use (d, γ) to represent our scheduling policy.

Algorithm 1 Threshold-based Power-of-d Scheduling Policy

Given positive integer d and non-negative integer γ, at each scheduling instant t,
(1) The scheduler issues d upload commends to d randomly selected physical entities.
(2) Each entity that receives the command will report its state to the scheduler only if its VAoI, $Q_n(t) \geq \gamma$.
(3) Among the physical entities that report their states, the scheduler selects the physical entity n with the maximum $Q_n(t)$ for the transmission.

From the definition of the Threshold-based power-of-d scheduling policy, we know the transition rate $q_{m,0}^{(d,\gamma)} = 0$ for $m < \gamma$, then the Markov Chain becomes Fig. 6.
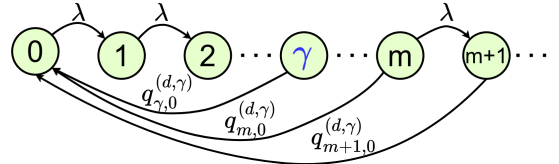

Fig. 6: The VAoI Markov Chain of a single physical entity in the large-system limit.

Proposition 2. *Under the Threshold-based Power-of-d scheduling policy, given the algorithm parameters d and γ as well as the system parameters λ and μ:*

(1) The distribution of the VAoI of the large-scale system in steady state is uniquely determined by the sequence of tail probabilities $\{S_m^{(d,\gamma)}\}_{m \in \mathbb{Z}_+}$, where $S_m^{(d,\gamma)}$ for integer $m \geq 0$ can be calculated iteratively using the equation

$$\begin{cases} \mu[1 - (1 - S_m^{(d,\gamma)})^d] + S_m^{(d,\gamma)}\lambda = S_{m-1}^{(d,\gamma)}\lambda, m > \gamma \\ S_m^{(d,\gamma)} = 1 - m\pi_0^{(d,\gamma)}, m \leq \gamma \end{cases} \tag{11}$$

where $\pi_0^{(d,\gamma)}$ is given by solving

$$\mu[1 - (\gamma\pi_0^{(d,\gamma)})^d] = \lambda\pi_0^{(d,\gamma)}. \tag{12}$$

Moreover, the impact of d and γ is given as follows:

(a) For a fixed $d \in \mathbb{Z}_+$, $S_m^{(d,\gamma)} < S_m^{(d,\gamma+1)} \quad \forall m, \gamma \in \mathbb{Z}_+$.
(b) For a fixed $\gamma \in \mathbb{Z}_+$, $S_m^{(d+1,\gamma)} < S_m^{(d,\gamma)} \quad \forall m, d \in \mathbb{Z}_+$.

Therefore, by the tail-sum formula $\overline{Q}^{(d,\gamma)} = \sum_{m=1}^{\infty} S_m^{(d,\gamma)}$,

$$\overline{Q}^{(d+1,\gamma)} < \overline{Q}^{(d,\gamma)} \text{ and } \overline{Q}^{(d,\gamma)} < \overline{Q}^{(d,\gamma+1)} \quad \forall d, \gamma \in \mathbb{Z}_+. \tag{13}$$

(2) The average communication overhead is given by

$$\overline{C}^{(d,\gamma)} = dS_\gamma^{(d,\gamma)} = d(1 - \gamma\pi_0^{(d,\gamma)}) \tag{14}$$

Moreover, for a fixed $d \in \mathbb{Z}_+$, the impact of γ is given as,

$$\overline{C}^{(d,\gamma)} > \overline{C}^{(d,\gamma+1)} \quad \forall \gamma \in \mathbb{Z}_+ \tag{15}$$

and for a fixed $\gamma \in \mathbb{Z}_+$, the impact of d is given as,

$$\frac{\overline{C}^{(d,\gamma)}}{d} > \frac{\overline{C}^{(d+1,\gamma)}}{d+1} \quad \forall \gamma \in \mathbb{Z}_+. \tag{16}$$

Proof. For the Threshold-based Power-of-d scheduling policy, the threshold γ can be seen as the boundary point, then the entire Markov Chain can be analyzed from two perspectives according to two types of balance equations:

(i) For $m < \gamma$: $\pi_{m-1}^{(d,\gamma)} \lambda = \pi_m^{(d,\gamma)} \lambda \to \pi_{m-1}^{(d,\gamma)} = \pi_m^{(d,\gamma)}$.

(ii) For $m \geq \gamma$: $\mu[1 - (1 - S_m^{(d,\gamma)})^d] + \lambda S_m^{(d,\gamma)} = \lambda S_{m-1}^{(d,\gamma)}$.

where for $m \geq \gamma$, the equation can be derived following the same analytical process as in Proposition 1. Based on these observations, we can express $S_m^{(d,\gamma)}$ for $m \leq \gamma$ as:

$$S_m^{(d,\gamma)} = 1 - \sum_{j=0}^{m-1} \pi_j^{(d,\gamma)} = 1 - m\pi_0^{(d,\gamma)}. \tag{17}$$

By substituting $S_\gamma^{(d,\gamma)}$ and $S_{\gamma-1}^{(d,\gamma)}$ into balance equation (ii), we can get Eq. (12).

Next we would like to show (a) for a fixed $m \leq \gamma$. Define the function $f_0^{(d,\gamma)} : (0,1) \to \mathbb{R}$ as

$$f_0^{(d,\gamma)}(x) = \mu[1 - (\gamma x)^d] - \lambda x. \tag{18}$$

It's easy to check at that $f_0^{(d,\gamma)}$ is invertible and we denote its inverse by $[f_0^{(d,\gamma)}(x)]^{-1}$. It's also easy to check that the function is strictly decreasing and that its range contains 0. By setting $x = [f_0^{(d,\gamma)}(0)]^{-1} = \pi_0^{(d,\gamma)}$. Notice that $f_0^{(d,\gamma+1)}(x) < f_0^{(d,\gamma)}(x) = 0$. It follows that $\pi_0^{(d,\gamma+1)} = [f_0^{(d,\gamma+1)}(0)]^{-1} < x$ since the function $f_0^{(d,\gamma)}$ is strictly decreasing. Then from the Eq. (17), we can get the inequality,

$$\pi_0^{(d,\gamma+1)} < \pi_0^{(d,\gamma)} \implies S_m^{(d,\gamma)} < S_m^{(d,\gamma+1)} \quad \forall m \leq \gamma \tag{19}$$

Next, we show (a) for $m \geq \gamma + 1$ by induction. For each $m = 1, 2, \ldots$ define the function $f_{m+1}^{(d,\gamma)} : (0,1) \to \mathbb{R}$ given by

$$f_{m+1}^{(d,\gamma)}(x) = \frac{\mu}{\lambda}\left(1 - (1-x)^d\right) + x - S_m^{(d,\gamma)}. \tag{20}$$

Define its inverse as $[f_{m+1}^{(d,\gamma)}(x)]^{-1}$. Then we need to show that

$$S_m^{(d,\gamma+1)} = [f_m^{(d,\gamma+1)}(0)]^{-1} > [f_m^{(d,\gamma)}(0)]^{-1} = S_m^{(d,\gamma)}. \tag{21}$$

First, we check the base case when $m = \gamma + 1$. From Eq. (11), we can obtain $S_{\gamma+1}^{(d,\gamma)}$ by solving

$$\frac{\mu}{\lambda}[1 - (1 - S_{\gamma+1}^{(d,\gamma)})^d] + S_{\gamma+1}^{(d,\gamma)} = S_\gamma^{(d,\gamma)} \tag{22}$$

and obtain $S_{\gamma+1}^{(d,\gamma+1)}$ by solving

$$S_{\gamma+1}^{(d,\gamma+1)} = 1 - (\gamma + 1)\pi_0^{(d,\gamma+1)}. \tag{23}$$

Then we can get the following inequality,

$$\begin{aligned}
f_{\gamma+1}^{(d,\gamma)}(S_{\gamma+1}^{(d,\gamma+1)}) &= \frac{\mu}{\lambda}\left[1 - [(\gamma+1)\pi_0^{(d,\gamma+1)}]^d\right] \\
&\quad + \gamma[\pi_0^{(d,\gamma)} - \pi_0^{(d,\gamma+1)}] - \pi_0^{(d,\gamma+1)} \tag{24}
\end{aligned}$$

$$\overset{(c)}{=} \gamma[\pi_0^{(d,\gamma)} - \pi_0^{(d,\gamma+1)}] \overset{(d)}{>} 0$$

where (c) is due to Eq. (12) and (d) is due to Eq. (19). It is easy to check that $f_{\gamma+1}^{(d,\gamma)}(x)$ is a monotonically increasing function, which means $x = [f_{\gamma+1}^{(d,\gamma)}(0)]^{-1} < S_{\gamma+1}^{(d,\gamma+1)}$, so we get $S_{\gamma+1}^{(d,\gamma)} < S_{\gamma+1}^{(d,\gamma+1)}$ and therefore Eq. (21) holds for $m = \gamma + 1$. Now suppose Eq. (21) holds for an arbitrary $m > \gamma + 1$ and set $x = [f_{m+1}^{(d,\gamma)}(0)]^{-1}$. Then we have $f_{m+1}^{(d,\gamma)}(x) = 0$, and

$$f_{m+1}^{(d,\gamma+1)}(x) = \frac{\mu}{\lambda}\left(1 - (1-x)^d\right) + x - S_m^{(d,\gamma+1)} < 0 \tag{25}$$

Then $[f_{m+1}^{(d,\gamma+1)}(0)]^{-1} > [f_{m+1}^{(d,\gamma)}(0)]^{-1}$ since the function is monotonically increasing. Therefore Eq. (21) holds for all $m > \gamma + 1$ and (a) is proven.

Fix $\gamma \in \mathbb{Z}_+$. To prove part (b), we begin with $m \leq \gamma$. We first need to prove that $\pi_0^{(d,\gamma)} < \pi_0^{(d+1,\gamma)}$ by contradiction. Assume $\pi_0^{(d,\gamma)} \geq \pi_0^{(d+1,\gamma)}$. If $\pi_0^{(d,\gamma)} = \pi_0^{(d+1,\gamma)}$, then Eq. (12) clearly doesn't hold and we arrive at a contradiction. Then we proceed assuming $\pi_0^{(d,\gamma)} > \pi_0^{(d+1,\gamma)}$. Note that since the right-hand side of Eq. (12) is positive, $\gamma\pi_0^{(d,\gamma)} < 1$. Then from d to $d+1$, the right-hand side decreases, but the left-hand side increases and we arrive at a contradiction. Then we conclude that $\pi_0^{(d,\gamma)} < \pi_0^{(d+1,\gamma)}$. From Eq. (17), we have that

$$\pi_0^{(d+1,\gamma)} < \pi_0^{(d,\gamma)} \implies S_m^{(d+1,\gamma)} < S_m^{(d,\gamma)} \quad \forall m \leq \gamma. \tag{26}$$

To show that (b) holds for $m > \gamma$, we need to use induction. We omit this part since it's the same as in the proof of Proposition 1 which can be found in our technical report [28], except taking $m = \gamma + 1$ as the base case.

Proceeding to part (2), fix γ and note that the probability that each entity reports its state is $S_\gamma^{(d,\gamma)}$, and d entities are selected. Then the number of reporting entities follows a Binomial $(d, S_\gamma^{(d,\gamma)})$ distribution. Also recall from Eq. (17) that $S_\gamma^{(d,\gamma)} = 1 - \gamma\pi_0^{(d,\gamma)}$. Then Eq. (14) holds. Recall from Eq. (19) that $\pi_0^{(d,\gamma+1)} < \pi_0^{(d,\gamma)}$. Rearranging Eq. (12) gives

$$\gamma\pi_0^{(d,\gamma)} = \left(1 - \frac{\lambda\pi_0^{(d,\gamma)}}{\mu}\right)^{\frac{1}{d}} < \left(1 - \frac{\lambda\pi_0^{(d,\gamma+1)}}{\mu}\right)^{\frac{1}{d}} \tag{27}$$

and therefore $\gamma\pi_0^{(d,\gamma)} < (\gamma+1)\pi_0^{(d,\gamma+1)}$. Then Eq. (15) holds. Finally, Eq. (16) holds from Eq. (14) and Eq. (26). $\qquad \square$

Remark 2. *The results are intuitive. Regarding the average VAoI, increasing γ reduces the probability of a physical entity being scheduled, because it must have a VAoI of at least γ to be selected. This leads to less frequent state transmissions, ultimately resulting in a higher average VAoI. For the average communication overhead, since only physical entities with a VAoI greater than or equal to γ are scheduled, the probability of this event occurring is given by $S_\gamma^{(d,\gamma)}$ as defined earlier.*

From an expectation perspective, the average overhead is given by the total number d multiplied by the probability $S_\gamma^{(d,\gamma)}$. Additionally, we can conclude that the Threshold-based Power-of-d scheduling policy can reduce the average communication overhead compared to the Power-of-d scheduling policy by

$$\frac{\overline{C}^{(d)} - \overline{C}^{(d,\gamma)}}{\overline{C}^{(d)}} = 1 - S_\gamma^{(d,\gamma)} = \gamma\pi_0^{(d,\gamma)}. \quad (28)$$

When $\gamma = 0$, it results $\overline{C}^{(d)} = \overline{C}^{(d,\gamma)}$, then our policy performs equivalently to the Power-of-d scheduling policy.

V. SIMULATION RESULTS

In this section, we first validate the accuracy of the mean-field analysis thus proving the rationality of our assumption. Then we compare the overall performance of the Threshold-based Power-of-d scheduling policy with other scheduling policies to explore the performance improvements achieved by our algorithm. All results of comparative experiments are conducted with $N = 2000$ physical entities, total time of $T = 10^7$, and server parameter $\mu = 1$.

A. Validation of the Mean-Field Analysis

In this subsection, we verify the theoretical accuracy of the mean-field analysis. For each specific setting, we calculate the numerical result of performance metrics using an event-driven simulation. Specifically, we generate a series of events, including "arrival" (a change in the VAoI of any physical entity) and "service" (when the twin world finishes one service and the scheduler begins scheduling a physical entity). We track the number of physical entities scheduled at each scheduling instant and analyze the dynamics of each physical entity's VAoI over time, until the total time limit is reached. The precise theoretical values are calculated by a computer solving equations.

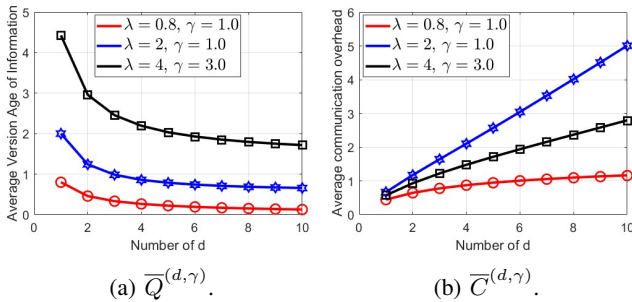(a) $\overline{Q}^{(d,\gamma)}$. (b) $\overline{C}^{(d,\gamma)}$.

Fig. 7: Experimental results of Threshold-based policy.

The lines in Fig. 7 and Fig. 8 represent the simulation results, while the markers correspond to the theoretical outcomes. It is evident that the simulation results align closely with the theoretical analysis across various scene settings. This strong agreement validates the accuracy of the mean-field analysis and our assumption, demonstrating its reliability in modeling the behavior of large-scale DT systems.

Fig. 9 demonstrates that the simulation results converge to the theoretical outcomes under different settings as the total
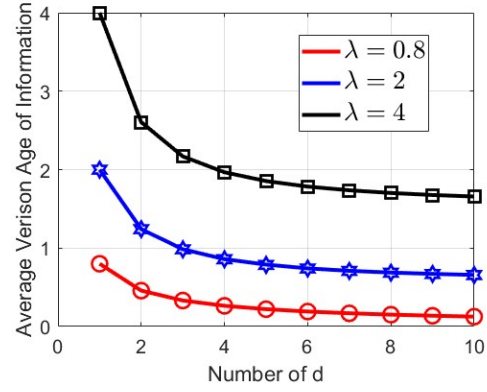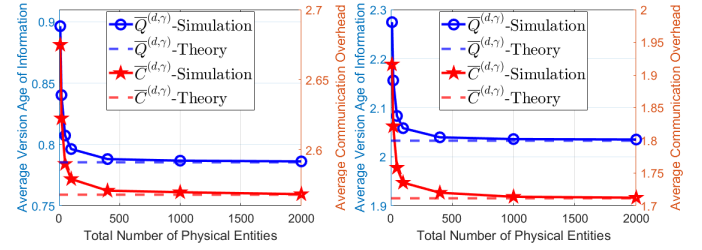
Fig. 8: Experimental results of Power-of-d scheduling policy.

(a) $\lambda = 2$, $d = 5$, and $\gamma = 1$. (b) $\lambda = 4$, $d = 5$, and $\gamma = 3$.

Fig. 9: Convergence of experiments to theory as $N \to \infty$.

number of physical entities N increases, and the theoretical analysis is accurate even for $N = 500$. This behavior aligns with the large-system limit.

B. Overall Performance Comparison

In this subsection, we compare the overall performance of the Threshold-based Power-of-d scheduling policy with other scheduling policies, with a particular focus on the Power-of-d scheduling policy. Fig. 10 shows the performance of different policies under the setting with $\lambda = 0.8$ and a threshold of $\gamma = 1.0$. From Fig. 10a (average VAoI), we observe that our policy achieves a performance comparable to that of the Power-of-d scheduling policy. Additionally, we note that $\overline{Q}^{(\pi)}$ decreases as d increases, which can be attributed to the expanded likelihood that the scheduler serves physical entities with a large VAoI. In terms of $\overline{C}^{(\pi)}$, Fig. 10b highlights the significant performance improvement (reduced average communication overhead) of our policy. Notably, our policy achieves the same $\overline{Q}^{(\pi)}$ as the Power-of-d scheduling policy with only one-twentieth of the average communication overhead at $d = 30$.

Fig. 11 presents the performance of different policies under the setting with $\lambda = 2.0$ and $\gamma = 2.0$. While Fig. 11b clearly shows a significant reduction in communication overhead for our policy compared to the Power-of-d scheduling policy, we observe a slight increase in the average VAoI from Fig. 11a. This outcome is consistent with our theoretical analysis, which shows that the reduction in $\overline{C}^{(\pi)}$ comes at the expense of a slight increase in $\overline{Q}^{(\pi)}$.
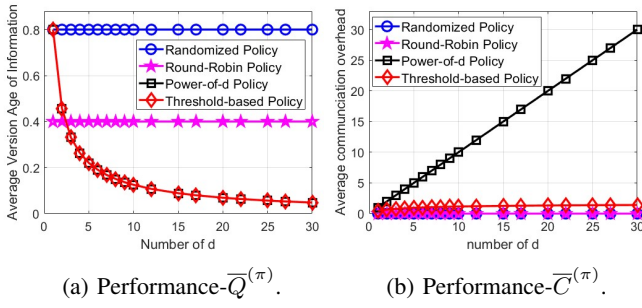
(a) Performance-$\overline{Q}^{(\pi)}$. (b) Performance-$\overline{C}^{(\pi)}$.

Fig. 10: Performance comparison under $\lambda = 0.8$ and $\gamma = 1.0$.

(a) Performance-$\overline{Q}^{(\pi)}$. (b) Performance-$\overline{C}^{(\pi)}$.
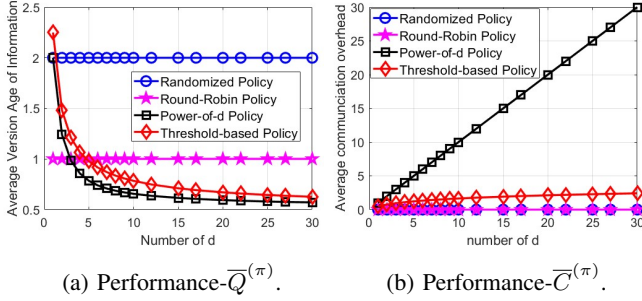
Fig. 11: Performance comparison under $\lambda = 2.0$ and $\gamma = 2.0$.

VI. CONCLUSION

In this paper, we studied the performance of the average *Version Age of Information* (VAoI) and average communication overhead in large-scale Digital Twin (DT) systems with numerous physical entities and a shared communication channel. We analyzed the steady state performance in the asymptotic limit of large-scale DT systems, where the number of physical entities goes to infinity. We first analyzed the Randomized and Round-Robin scheduling policy and showed the motivation according to compare them with the Max-VAoI scheduling policy. Then through mean-field analysis, we derived the steady-state distribution of each physical entity's VAoI under Power-of-d scheduling policy. In particular, we proposed a Threshold-based Power-of-d scheduling policy, which builds upon the Power-of-d scheduling policy and threshold to optimize communication resource usage. Our policy demonstrates a significant reduction in average communication overhead, albeit at the cost of a slight increase in the average VAoI. Finally, numerical results across different scenario settings validate the accuracy of our theoretical analysis.

REFERENCES

[1] National Academy of Engineering and National Academies of Sciences, Engineering, and Medicine, *Foundational research gaps and future directions for Digital Twins*. Washington, DC: The National Academies Press, 2024.

[2] L. U. Khan, W. Saad, D. Niyato, Z. Han, and C. S. Hong, "Digital-Twin-enabled 6G: Vision, architectural trends, and future directions," *IEEE Communications Magazine*, vol. 60, no. 1, pp. 74–80, Jan 2022.

[3] F. Tao, H. Zhang, A. Liu, and A. Y. Nee, "Digital Twin in industry: State-of-the-art," *IEEE Transactions on industrial informatics*, vol. 15, no. 4, pp. 2405–2415, 2018.

[4] F. Tao, M. Zhang, J. Cheng, and Q. Qi, "Digital Twin workshop: a new paradigm for future workshop," *Computer Integrated Manufacturing Systems*, vol. 23, no. 1, pp. 1–9, 2017.

[5] G. White, A. Zink, L. Codecá, and S. Clarke, "A Digital Twin Smart City for citizen feedback," *Cities*, vol. 110, p. 103064, 2021.

[6] Z. Wang, K. Han, and P. Tiwari, "Digital Twin-assisted cooperative driving at non-signalized intersections," *IEEE Transactions on Intelligent Vehicles*, vol. 7, no. 2, pp. 198–209, 2021.

[7] F. Jiang, L. Ma, T. Broyd, W. Chen, and H. Luo, "Digital Twin enabled sustainable urban road planning," *Sustainable Cities and Society*, vol. 78, p. 103645, 2022.

[8] Y. Wu, K. Zhang, and Y. Zhang, "Digital Twin networks: A survey," *IEEE Internet of Things Journal*, vol. 8, no. 18, pp. 13 789–13 804, 2021.

[9] S. Kaul, R. Yates, and M. Gruteser, "Real-time status: How often should one update?" in *2012 Proceedings IEEE INFOCOM*. IEEE, 2012, pp. 2731–2735.

[10] R. D. Yates and S. Kaul, "Real-time status updating: Multiple sources," in *2012 IEEE International Symposium on Information Theory Proceedings*. IEEE, 2012, pp. 2666–2670.

[11] M. Moltafet, M. Leinonen, and M. Codreanu, "Average AoI in multi-source systems with source-aware packet management," *IEEE Transactions on Communications*, vol. 69, no. 2, pp. 1121–1133, 2020.

[12] R. D. Yates and S. K. Kaul, "The Age of Information: Real-time status updating by multiple sources," *IEEE Transactions on Information Theory*, vol. 65, no. 3, pp. 1807–1827, 2018.

[13] R. V. Ramakanth, V. Tripathi, and E. Modiano, "Monitoring correlated sources: AoI-based scheduling is nearly optimal," *IEEE Transactions on Mobile Computing*, 2024.

[14] L. Huang and E. Modiano, "Optimizing Age-of-Information in a multi-class queueing system," in *2015 IEEE international symposium on information theory (ISIT)*. IEEE, 2015, pp. 1681–1685.

[15] R. Li, A. Eryilmaz, and B. Li, "Throughput-optimal wireless scheduling with regulated inter-service times," in *2013 Proceedings IEEE INFOCOM*. IEEE, 2013, pp. 2616–2624.

[16] B. Li, R. Li, and A. Eryilmaz, "Throughput-optimal scheduling design with regular service guarantees in wireless networks," *IEEE/ACM Transactions on Networking*, vol. 23, no. 5, pp. 1542–1552, 2014.

[17] Y. Sun, I. Kadota, R. Talak, and E. Modiano, *Age of Information: A new metric for information freshness*. Springer Nature, 2022.

[18] R. D. Yates, "The Age of Gossip in Networks," in *2021 IEEE International Symposium on Information Theory (ISIT)*. IEEE, 2021, pp. 2984–2989.

[19] M. Bramson, Y. Lu, and B. Prabhakar, "Randomized load balancing with general service time distributions," *ACM SIGMETRICS performance evaluation review*, vol. 38, no. 1, pp. 275–286, 2010.

[20] N. D. Vvedenskaya, R. L. Dobrushin, and F. I. Karpelevich, "Queueing system with selection of the shortest of two queues: An asymptotic approach," *Problemy Peredachi Informatsii*, vol. 32, no. 1, pp. 20–34, 1996.

[21] M. Mitzenmacher, "The power of two choices in randomized load balancing," *IEEE Transactions on Parallel and Distributed Systems*, vol. 12, no. 10, pp. 1094–1104, 2001.

[22] R. Sitaraman, "The power of two random choices: A survey of techniques and results," 2001.

[23] Y. Sun, Y. Polyanskiy, and E. Uysal, "Sampling of the Wiener process for remote estimation over a channel with random delay," *IEEE Transactions on Information Theory*, vol. 66, no. 2, pp. 1118–1135, 2019.

[24] V. Tripathi and E. Modiano, "A Whittle Index approach to minimizing functions of Age of Information," in *2019 57th Annual Allerton Conference on Communication, Control, and Computing (Allerton)*. IEEE, 2019, pp. 1160–1167.

[25] J. Yun, C. Joo, and A. Eryilmaz, "Optimal real-time monitoring of an information source under communication costs," in *2018 IEEE Conference on Decision and Control (CDC)*. IEEE, 2018, pp. 4767–4772.

[26] Q.-L. Li, G. Dai, J. C. Lui, and Y. Wang, "The mean-field computation in a supermarket model with server multiple vacations," *Discrete Event dynamic systems*, vol. 24, pp. 473–522, 2014.

[27] B. Li, A. Ramamoorthy, and R. Srikant, "Mean-field analysis of coding versus replication in large data storage systems," *ACM Transactions on Modeling and Performance Evaluation of Computing Systems (TOMPECS)*, vol. 3, no. 1, pp. 1–28, 2018.

[28] "Low-overhead scheduling for synchronization in large-scale digital twin systems." [Online]. Available: https://gitlab.com/senc-zifan/dt-threspot.git

APPENDIX A
PROOF OF LEMMA 1

We set δ as a small time interval, then $q_{m,0}^{(d)}\delta$ is the average number of physical entities with *Version AoI* of m is scheduled in a small time interval δ, which can also be represented as $N\mu\delta \times \Pr\{A\} \times \Pr\{B\}$, where event A and B are defined as follows:

$$A \triangleq \{\text{Physical entity } n \text{ is considered for scheduling}\} \quad (29)$$

$$B \triangleq \{n \text{ is scheduled } \mid n \text{ is considered for scheduling} \\ , Q_n(t) = m\} \quad (30)$$

where event A indicator is i.i.d. across scheduling instants and follows a Hypergeometric$(N, 1, d)$ distribution. Event B can also be explained as the physical entity n has the maximal $Q_n(t)$ among the selected physical entities given its state is m. Then,

$$\Pr\{n \text{ is scheduled } \mid Q_n(t) = m\} = \Pr\{A\} \times \Pr\{B\}. \quad (31)$$

According to the Power-of-d scheduling policy rule, the indicator of event A is $\mathbf{1}\{n$ is considered for scheduling$\} \sim$ Hypergeometric$(N, 1, d)$, we have

$$\Pr\{A\} = \mathbb{E}[\mathbf{1}\{n \text{ is considered for scheduling}\}] = \frac{d}{N}. \quad (32)$$

$$\Pr\{B\} = \frac{1}{d}(\pi_m^{(d)})^{d-1} + \binom{d-1}{1}\frac{1}{d-1}(\pi_m^{(d)})^{d-2}(1 - S_m^{(d)}) + \\ \binom{d-1}{2}\frac{1}{d-2}(\pi_m^{(d)})^{d-3}(1 - S_m^{(d)})^2 + \cdots + (1 - S_m^{(d)})^{d-1} \\ = \frac{1}{d}\sum_{i=1}^{d}\binom{d}{i-1}(\pi_m^{(d)})^{d-i}(1 - S_m^{(d)})^{i-1} \quad (33)$$

Subscribing Eq. (32) and Eq. (33) to the equality, we can get,

$$q_{m,0}^{(d)}\delta = N\mu\delta\frac{d}{N}\frac{1}{d}\sum_{i=1}^{d}\binom{d}{i-1}(\pi_m^{(d)})^{d-i}(1 - S_m^{(d)})^{i-1} \\ = \mu\delta\Big[\frac{1}{\pi_m^{(d)}}\sum_{i=1}^{d}\binom{d}{i-1}(\pi_m^{(d)})^{d-i+1}(1 - S_m^{(d)})^{i-1}\Big] \\ = \frac{\mu\delta}{\pi_m^{(d)}}\Big[\sum_{i=1}^{d+1}\binom{d}{i-1}(\pi_m^{(d)})^{d-i+1}(1 - S_m^{(d)})^{i-1} \\ - (1 - S_m^{(d)})^d\Big] \\ = \frac{\mu\delta}{\pi_m^{(d)}}\Big[(1 - S_m^{(d)} + \pi_m^{(d)})^d - (1 - S_m^{(d)})^d\Big] \\ = \frac{\mu\delta}{\pi_m^{(d)}}\Big[(1 - S_{m+1}^{(d)})^d - (1 - S_m^{(d)})^d\Big] \quad (34)$$

APPENDIX B
PROOF FOR EQ. (5)

To finish proving Eq. (5), it remains to show that (10) admits a unique solution and that $S_m^{(d+1)} < S_m^{(d)}$ for all $m, d \in \mathbb{Z}_+$. For each $m, d \in \mathbb{Z}_+$, define the function $f_m^{(d)} : (0, 1) \to \mathbb{R}$ given by

$$f_m^{(d)}(x) = \frac{\mu}{\lambda}\left(1 - (1 - x)^d\right) + x - S_{m-1}^{(d)}. \quad (35)$$

It's easy to check that $f_m^{(d)}$ is invertible and we denote its inverse by $[f_m^{(d)}]^{-1}$. It's also easy to check that the function is strictly increasing and that its range contains 0. Then according to Eq. (10) and noting that $S_0^{(d)} = 1$, we can uniquely and iteratively calculate $S_1^{(d)} = [f_1^{(d)}]^{-1}(0)$, and then $S_2^{(d)} = [f_2^{(d)}]^{-1}(0)$, and so on.

It remains to show by induction that for a fixed $d \in \mathbb{Z}_+$, for all $m = 1, 2, \dots$ we have

$$S_m^{(d+1)} = [f_m^{(d+1)}]^{-1}(0) < [f_m^{(d)}]^{-1}(0) = S_m^{(d)}. \quad (36)$$

First, we check the base case $m = 1$ and set $x = [f_1^{(d)}]^{-1}(0) = S_1^{(d)}$. Then

$$f_1^{(d)}(x) = \frac{\mu}{\lambda}\left(1 - (1 - x)^d\right) + x - 1 = 0 \quad (37)$$

and $f_1^{(d+1)}(x) > f_1^{(d)}(x) = 0$ because $(1 - x)^d > (1 - x)^{d+1}$ for $x \in (0, 1)$. It follows that $S_m^{(d+1)} = [f_m^{(d+1)}]^{-1}(0) < x$ since $f_1^{(d+1)}(x) > 0$ and the function $f_1^{(d+1)}$ is monotonically increasing in x. So, (36) holds for $m = 1$.

Before proceeding to the inductive step, observe that

$$\frac{\mu}{\lambda}\left(1 - (1 - x)^{d+1}\right) + x - y > \frac{\mu}{\lambda}\left(1 - (1 - x)^d\right) + x - z \quad (38)$$

for all $x, y, z \in (0, 1)$ such that $y < z$. Now suppose (36) holds for an arbitrary m and fix $x = [f_{m+1}^{(d)}]^{-1}(0) = S_{m+1}^{(d)}$. Then $f_{m+1}^{(d+1)}(x) > f_{m+1}^{(d)}(x) = 0$ by (38) with $y = S_m^{(d+1)}$ and $z = S_m^{(d)}$. It follows that $S_{m+1}^{(d+1)} = [f_{m+1}^{(d+1)}]^{-1}(0) < x$ since $f_{m+1}^{(d+1)}(x) > 0$ and the function $f_{m+1}^{(d+1)}$ is monotonically increasing in x. So, (36) holds for $m + 1$ and therefore by induction, (36) holds for all $m = 1, 2, \dots$.

Therefore, we have the inequality,

$$\overline{Q}^{(d+1)} = \sum_{m=1}^{\infty}S_m^{(d+1)} = \sum_{m=1}^{\infty}[f_m^{(d+1)}]^{-1}(0) \\ < \overline{Q}^{(d)} = \sum_{m=1}^{\infty}S_m^{(d)} = \sum_{m=1}^{\infty}[f_m^{(d)}]^{-1}(0) \quad (39)$$

APPENDIX C
LOWER BOUND OF POWER-OF-d SCHEDULING POLICY

Lemma 2. *The average Version AoI of the Power-of-d scheduling policy can be lower bounded by λ and μ follows*

$$\overline{Q}^{(d)} \geq \frac{\lambda}{d\mu} \quad (40)$$

Proof. From Proposition 1, we can get the relationship between $S_m^{(d)}$ and $\pi_{m-1}^{(d)}$ for $m \geq 1$,

$$\mu[1 - (1 - S_m^{(d)})^d] = S_{m-1}^{(d)}\lambda - S_m^{(d)}\lambda = \lambda\pi_{m-1}^{(d)} \quad (41)$$

Then cumulatively summing the above equation we get,

$$\sum_{m=1}^{\infty} \mu[1-(1-S_m^{(d)})^d] = \lambda \rightarrow \sum_{m=1}^{\infty} [1-(1-S_m^{(d)})^d] = \frac{\lambda}{\mu} \quad (42)$$

Under the condition $S_m^{(d)} \in (0,1)$ and $d \geq 1$, we can get the equation by the Bernoulli's inequality,

$$(1-S_m^{(d)})^d \geq 1 - dS_m^{(d)} \quad (43)$$

Then we have,

$$\frac{\lambda}{\mu} = \sum_{m=1}^{\infty} [1-(1-S_m^{(d)})^d] \leq \sum_{m=1}^{\infty} dS_m^{(d)} \rightarrow \sum_{m=1}^{\infty} S_m^{(d)} \geq \frac{\lambda}{d\mu} \quad (44)$$

$\square$

APPENDIX D
PROOF OF LEMMA 3

Lemma 3. *For $x \geq 0$, there exists the inequality,*

$$\ln(1+x) \geq x - \frac{x^2}{2} \quad (45)$$

Proof. For $x \geq 0$, we set the function about x as

$$f(x) = \ln(1+x) - (x - \frac{x^2}{2}). \quad (46)$$

Then the first derivatives and the second derivatives are

$$\frac{df(x)}{dx} = \frac{1}{1+x} - 1 + x \quad (47)$$

$$\frac{d^2f(x)}{dx^2} = 1 - \frac{1}{(1+x)^2} \quad (48)$$

Note that Eq. (48) is always larger than or equal to 0 when $x \geq 0$, and Eq. (47) equals 0 when $x = 0$. Therefore, Eq. (46) is a monotonically increasing function with $f(0) = 0$. $\square$

APPENDIX E
UPPER BOUND OF POWER-OF-d SCHEDULING POLICY

Lemma 4. *With $d = 2^k$, where $k > 1$ is a positive integer. The average Version AoI of the "Power of d" scheduling policy can be upper bounded by λ and μ follows*

$$\overline{Q}^{(d)} < \frac{\lambda}{\exp\{1-S_1^{(d)} + \sum_{i=1}^{\log_2^{\frac{d}{2}}-1} \frac{1}{2}(1-S_1^{(d)})^{2^i}\}\mu} = \frac{\lambda}{\tilde{d}\mu} \quad (49)$$

Here $S_1^{(d)}$ can be calculated by the Proposition 1 with the initial condition $S_0^{(d)} = 1$.

Proof. Since $d = 2^k$, for each item of $\sum_{m=1}^{\infty}[1-(1-S_m^{(d)})^d]$, we can write it as,

$$[1-(1-S_m^{(d)})^d] = [1+(1-S_m^{(d)})^{\frac{d}{2}}][1+(1-S_m^{(d)})^{\frac{d}{4}}]\cdots$$
$$[1+(1-S_m^{(d)})^2][1+(1-S_m^{(d)})^{\frac{d}{d}}][1-(1-S_m^{(d)})^{\frac{d}{d}}]$$

$$= S_m^{(d)} \prod_{k=0}^{\log_2^{\frac{d}{2}}} [1+(1-S_m^{(d)})^{2^k}] \quad (50)$$

For the later repeated multiplication item, we can get the following inequality according to log operation,

$$\ln \prod_{k=0}^{\log_2^{\frac{d}{2}}} [1+(1-S_m^{(d)})^{2^k}] = \sum_{k=0}^{\log_2^{\frac{d}{2}}} \ln[1+(1-S_m^{(d)})^{2^k}]$$

$$\overset{(a)}{\geq} \sum_{k=0}^{\log_2^{\frac{d}{2}}} \{(1-S_m^{(d)})^{2^k} - \frac{1}{2}[(1-S_m^{(d)})^{2^k}]^2\}$$

$$= (1-S_m^{(d)}) + \sum_{k=1}^{\log_2^{\frac{d}{2}}} [\frac{1}{2}(1-S_m^{(d)})^{2^k}] - \frac{1}{2}(1-S_m^{(d)})^d$$

$$\overset{(b)}{\geq} (1-S_m^{(d)}) + \sum_{k=1}^{\log_2^{\frac{d}{2}}-1} [\frac{1}{2}(1-S_m^{(d)})^{2^k}] \quad (51)$$

Where (a) according to Lemma 3. For (b), we have $(1-S_m^{(d)}) \in (0,1)$, then we have $(1-S_m^{(d)})^{\frac{d}{2}} > (1-S_m^{(d)})^d$. By performing exponential operations on both sides of the above inequality, we can get

$$\prod_{k=0}^{\log_2^{\frac{d}{2}}} [1+(1-S_m^{(d)})^{2^k}] \geq \exp\{(1-S_m^{(d)}) + \sum_{k=1}^{\log_2^{\frac{d}{2}}-1} [\frac{1}{2}(1-S_m^{(d)})^{2^k}]\} \quad (52)$$

From the above analysis, we can derive,

$$\sum_{m=1}^{\infty} [1-(1-S_m^{(d)})^d] = \sum_{m=1}^{\infty} S_m^{(d)} \prod_{k=0}^{\log_2^{\frac{d}{2}}} [1+(1-S_m^{(d)})^{2^k}]$$

$$\geq \sum_{m=1}^{\infty} S_m^{(d)} \exp\{(1-S_m^{(d)}) + \sum_{k=1}^{\log_2^{\frac{d}{2}}-1} [\frac{1}{2}(1-S_m^{(d)})^{2^k}]\}$$

$$> \exp\{(1-S_1^{(d)}) + \sum_{k=1}^{\log_2^{\frac{d}{2}}-1} [\frac{1}{2}(1-S_1^{(d)})^{2^k}]\} \sum_{m=1}^{\infty} S_m^{(d)} \quad (53)$$

In the final step, as m increases, $S_m^{(d)}$ decreases, making the exponential term a monotonically increasing function. $\square$

APPENDIX F
DISTRIBUTION OF THE NUMBER OF POISSON POINTS OVER AN ERLANG INTERVAL

Lemma 5. *For $\lambda, \mu > 0$ and $k \in \mathbb{Z}_+$, suppose $U(T) \sim Poisson(\lambda T)$ for any $T > 0$ and $T_k \sim Erlang(k, \mu)$. Then $U(T_k) \sim NB\left(k, \frac{\mu}{\lambda+\mu}\right)$.*

Proof. by the law of total probability,

$$\Pr\{U(T_k) = u\} = \int_0^\infty \Pr\{U(T_k) = u \mid T_k = t\} \frac{\mu^k t^{k-1} e^{-\mu t}}{(k-1)!} dt$$

$$= \int_0^\infty \left(\frac{(\lambda t)^u e^{-\lambda t}}{u!}\right) \frac{\mu^k t^{k-1} e^{-\mu t}}{(k-1)!} dt$$

$$= \frac{\lambda^u \mu^k}{u!(k-1)!} \int_0^\infty t^{u+k-1} e^{-(\lambda+\mu)t} dt$$

$$\overset{(a)}{=} \frac{\lambda^u \mu^k}{u!(k-1)!} (\lambda+\mu)^{-(u+k)} \Gamma(u+k)$$

$$= \frac{\lambda^u \mu^k (u+k-1)!}{u!(k-1)!(\lambda+\mu)^{(u+k)}}$$

$$= \underbrace{\binom{u+k-1}{u} \left(\frac{\lambda}{\lambda+\mu}\right)^u \left(\frac{\mu}{\lambda+\mu}\right)^k}_{\text{PMF of a NB}\left(k, \frac{\mu}{\lambda+\mu}\right) \text{ distributed random variable}}$$

$$\tag{54}$$

where (a) can be shown by introducing the change of variables $s = (\lambda+\mu)t$. □